Pol. J. Environ. Stud. Vol. 23, No. 3 (2014), 783-792

Original Research

Adsorption Behavior of Acid Bordeaux B from Aqueous Solution onto Waste Biomass of *Enteromorpha prolifera*

Yongfu Li, Fanping Meng*, You Zhou

Key Laboratory of Environmental Science and Ecology, Ministry of Education,
Ocean University of China, Qingdao 266100, China

Received: 30 June 2013
Accepted: 17 February 2014

Abstract

Enteromorpha prolifera green algae is the main species that causes green tide in China's Yellow Sea. To effectively realize the resourceful utilization of this biomass, batch experiments were carried out to investigate factors that impact the Acid Bordeaux B (ABB) absorption of *E. prolifera* powder, such as exposure time, pH, adsorbent dose, and oscillation frequency. The dye adsorption onto adsorbent was confirmed by Fourier transform infrared spectroscopy (FTIR). Results showed that amide, hydroxy, carboxylate, and C-O groups were involved in the adsorption process. The treatment conditions for dye concentration of 100 $mg \cdot L^{-1}$ were optimized: contact time 60 min, pH value 4 to 9, water temperature 303 to 313 K, adsorbent dosage 0.25 $g \cdot L^{-1}$ and oscillation frequency 150 rpm. Equilibrium data were analyzed by using the Freundlich and Langmuir models. The data fit well in both models. The maximum equilibrium adsorption capacity calculated by the Langmuir equation was 1,111.11-3,333.33 $mg \cdot g^{-1}$. To clarify the sorption kinetic, the fitness of the Pseudo-first-order model, the Pseudo-second-order model, and the intra-particle diffusion model were tested, showing that the pseudo-second order model was suitable to describe the adsorption process. The sorption process was complex, and both the boundary of liquid film and intra-particle diffusion contributed to the rate-determining step. Thermodynamic parameters (e.g. ΔG^0, ΔH^0, and ΔS^0) were calculated, which implied the exothermic and spontaneous nature of biosorption as well as the type of adsorption (physisorption). Results illustrate that the removal ratio from the wastewater with 100 $mg \cdot L^{-1}$ ABB reached 90.86%, indicating that *E. prolifera* could be a potential biosorbent used for the removal of ABB from industrial effluents.

Keywords: biosorption, *Enteromorpha prolifera*, Acid Bordeaux B, Dye removal, modeling

Introduction

Dyes have been used extensively in many industries, including textile, leather, plastics, paper, pharmacy, food, cosmetics, etc. [1-3]. The effluents of these industries are greatly colored with high quantity of dyes and not easily degraded to safe dye concentrations. The discharging of these wastes in the environment can be extremely deleterious [4-7].

*e-mail: fanpingm@126.com

Many treatment methods have been applied for the removal of dyes from wastewater, including adsorption processes, photodegration, sonochemical degradation, flocculation-flotation, membrane filtration, electrokinetic, coagulation, ozonation, oxidation, precipitation, and ion-exchange [8-14]. Among those techniques, the adsorption is considered to be the most effective [15]. Its efficiency depends on a dye's properties and adsorbent surface chemistry [16]. Activated carbon has been widely used to remove dyes from wastewater, but its use is restricted due

to its relatively high cost, the need for regeneration after use, and the decrease in adsorption efficiency after regeneration [17]. A great deal of attention has been paid to the employment of biosorbent materials, e.g. fungi [18], bacteria [19], algae [20], chitosan [21], and peat [22]. Recently, macroscopic algae have been considered as the dye sorbents such as brown seaweed Laminaria [23] and Sargassum [24], plus green algae Azolla [25, 26], Caulerpa [27-30], Spirogyra [31-34] and Enteromorpha [6, 35].

Enteromorpha, a green algae, frequently blooms in eutrophic sea areas and forms a dense mat, causing many negative influences on the aquatic ecosystem [36, 37]. Practically every year since 2007, green tide caused by *Enteromorpha prolifera* bloom occurred in the central and northern parts of the Yellow Sea. However, there is no effective method for synthetic utilization of this massive biomass. Using Enteromorpha as a bioabsorbent to remove dyes from the industrial effluents would be a "win-win" solution for both water pollution and biomass utilization [38]. Recent investigations have shown that the dried Enteromorpha was effective in removing the dyes dissolved in the aqueous solution such as Methylene Blue [35] and Acid Red 274 [6], proving its promising-prospect as an adsorption material.

In the present work, the removal of ABB from model solutions by the invasive *E. prolifera* was investigated in an aim to deal with the algae biomass. To the best of our knowledge, this is the first report of employing *E. prolifera* for ABB removal as an effective technology for material development.

Material and Methods

Preparation of Biosorbent

E. prolifera, was collected from the coast of Qingdao City, China (36º05′34.58″N, 120º28′21.47″E), in September 2009. The wet algal material was first washed with tap water to remove salt and epiphytes, and then washed with deionized water in order to remove the remaining salt. After drying at 105ºC for 48 h, the biomaterial powder form was crushed and screened to particle sizes in a range of 1-2 mm. The biosorbent was kept in a desiccator for sorption experimental test.

Determination of Possible Binding Sites by FTIR Analysis

The infrared spectra of natural and dye-laden adsorbents were analyzed through an FTIR spectrum (Bruker Tensor 27 FTIR Spectrometer, Germany). An FTIR spectrum of this material within the range of 4,000-500 cm^{-1} was chosen.

Preparation and Analysis of the Adsorbate

Acid Bordeaux B (ABB, $C_{20}H_{12}N_2Na_2O_7S_2$; CAS number 3567-69-9) was obtained from the Ceshin Chemical Company, Korea. The wavelength for maximum light absorption (λ_{max}) was initially examined for ABB to allow for effective measurement of dye concentration at λ_{max} 520 nm using a UV-Spectrophotometer (T6, Beijing, China). Stock dye solution was prepared in distilled water of 1.0 $g \cdot L^{-1}$.

Batch Adsorption Experiment

Adsorption studies were performed in a 250 ml Erlenmayer flask containing 100 ml of adsorption solution at 100 $mg \cdot L^{-1}$. Various experimental parameters including exposure time, initial solution pH, temperature, biosorbent dosage, and oscillation frequency were investigated due to their possible contributions to the biosorption of ABB on dried *E. prolifera*. The initial dye solutions with ABB concentration of 100 $mg \cdot L^{-1}$ were prepared by diluting the stock standard solution of 1.0 $g \cdot L^{-1}$. The pH was adjusted by using either diluted 0.1 N HCl or 0.1 N NaOH solutions. Known weight of adsorbent material was added into dye solution, taken in flasks, and then kept in a water bath oscillator at 150 rpm for 120 min to ensure equilibrium. The equilibrated solution was centrifuged at 5,000 rpm for 10 min. The removal efficiency of ABB (η, %) and the amount of ABB uptake per unit mass of adsorbent at t (Q_t, $mg \cdot g^{-1}$) and at equilibrium (Q_e, $mg \cdot g^{-1}$) were calculated through the following equations:

$$\eta = \frac{C_0 - C_e}{C_0} \times 100\% \quad (1)$$

$$Q_t = \frac{(C_0 - C_t) \times V}{M} \quad (2)$$

$$Q_e = \frac{(C_0 - C_e) \times V}{M} \quad (3)$$

...where:

η (%) – the removal efficiency of ABB

C_0, C_t, and C_e ($mg \cdot L^{-1}$) – the initial, time-t and equilibrium concentration of ABB in the solution, respectively

V (L) – the volume of solution

M (g) – the mass of adsorbent.

Results and Discussion

Investigations of Possible Biosorption Mechanism

Fig. 1 illustrated the FTIR spectra of dried *E. prolifera* and ABB-loaded biomass with its most abundant functional groups. As shown in Fig. 1 (a), the broad peak at 3,409.9 cm^{-1} was caused by the overlap of O–H and N–H stretching vibrations, indicating the presence of both surface free hydroxyl groups and chemisorbed water [26, 33, 39]. The bands at 2,924.2 cm^{-1} and 1,433.2 cm^{-1} corresponded to the C–H symmetric stretch of the methylene groups ($–CH_2$) and deformation vibration of methyl groups ($–CH_3$) [26]. The peak at 1,649.4 cm^{-1} was attributed to a C=O stretching vibration of carboxylate (–COO−) or an N–H deformation

vibration of amide I groups [26]. The peaks at 1,257.6 cm^{-1} and 1,037.0 cm^{-1} were due to the C–O stretching vibration of ketones, aldehydes and lactones or carboxyl groups [40]. S-O band was detected at 580.8 cm^{-1} [30]. Some shifts in wavenumbers from 3,409.9 cm^{-1} to 3,414.2 cm^{-1}, 2,924.2 cm^{-1} to 2,927.1 cm^{-1}, 1,037.0 cm^{-1} to 1,050.1 cm^{-1}, 1,433.2 cm^{-1} to 1,420.0 cm^{-1}, and 1,649.4 cm^{-1} to 1,645.5 cm^{-1}, were observed in the spectra of dried biomass of *E. prolifera* before and after use. These changes indicated interactions between biosorbent and ABB. Function groups on the surface of *E. prolifera* including amide, hydroxy, carboxylate and C–O groups could participate in ABB biosorption on the material [41]. Otherwise, compared to the unloaded biomass, a new peak at 1,340.9 cm^{-1} was observed in the spectrum of ABB-loaded biomass, which can be attributed to stretching the vibration of O=S=O [42]. This characteristic peak of ABB also implied the interaction between dried *E. prolifera* and dye.

Effect of Exposure Time: Sorption Dynamic

The exposure time affected the adsorption capacity of *E. prolifera* (Fig. 2). It can be seen that the sorption kinetics were very fast, i.e. in the first 5 mins most dye molecules were adsorbed. The equilibrium states were nearly reached at 60 mins. A plateau regime was then observed. A similar trend was observed for the adsorption of methylene blue on *E. prolifera* [35].

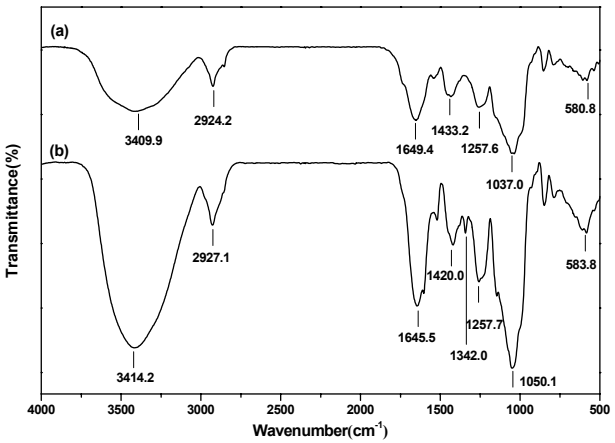

Fig. 1. FTIR spectra of dried pure *E. prolifera* (a) and dye laden *E. prolifera* (b).

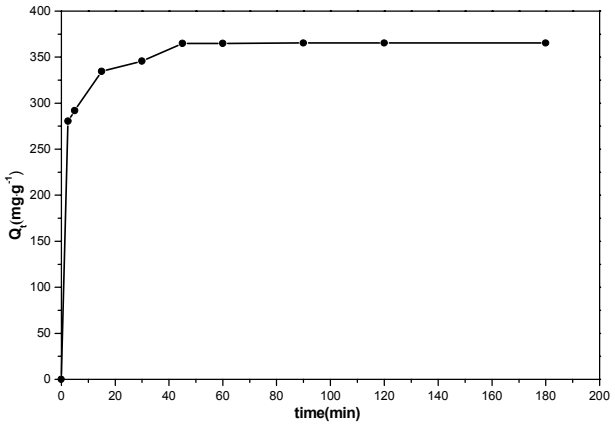

Fig. 2. Kinetic of ABB uptake by *E. prolifera* (Conditions: C_0 = 100 mg·L^{-1}, adsorbent dose = 0.25 g·L^{-1}, temperature = 293K, initial pH = 6.1, oscillation frequency = 150 rpm).

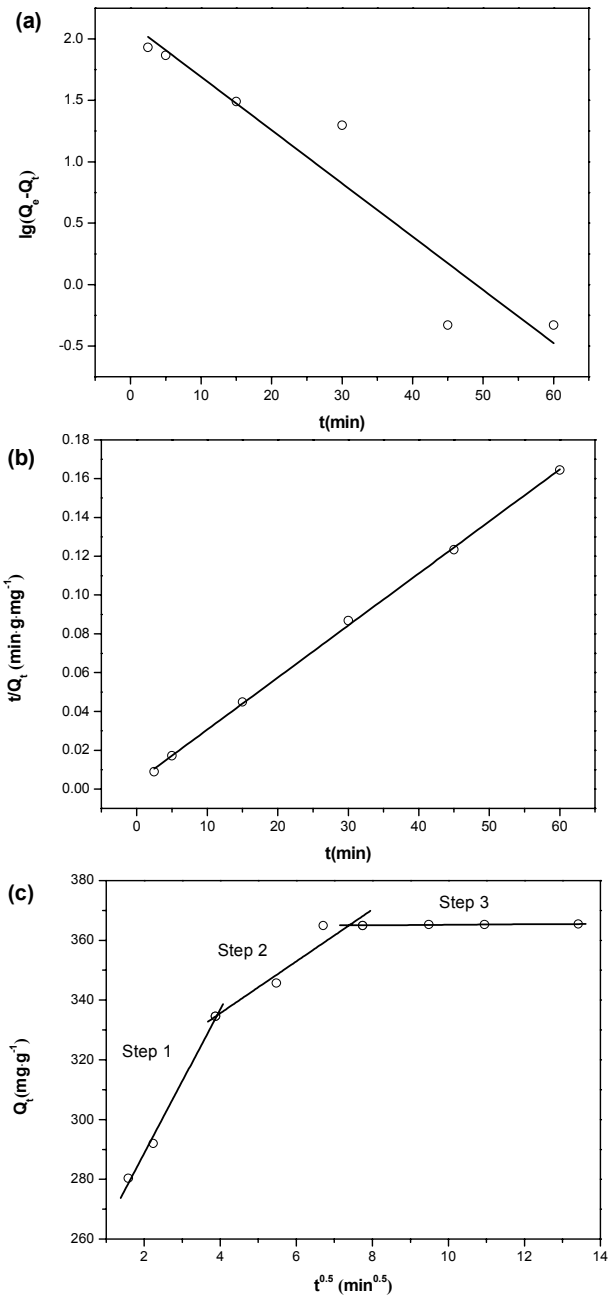

Fig. 3. Biosorption kinetics of ABB on dried *E. prolifera*. (a) the Pseudo-first-order model, (b) the Pseudo-Second-order model, and (c) the Intra-particle diffusion model.

Basically, the adsorption process can be separated into three stages:

(1) External diffusion or boundary layer diffusion
(2) Intra-particle mass diffusion
(3) Adsorption on the interior sites [43, 44].

Among these three phases, the last is an extremely fast process, in general, without a limited rate [45]. Three kinetic models were applied to fit the experimental data to examine the mechanism of biosorption of ABB on *E. prolifera*.

Table 1. Kinetics parameters of first-order, second-order models.

Parameters	C_0 (mg·L^{-1})	Q_e (mg·g^{-1})	Pseudo-first-order		Pseudo-second-order	
			k_1 (min^{-1})	R^2	k_2 (g·mg^{-1}·min^{-1})	R^2
Values	100	365	0.100	0.884	0.002	1.000

Pseudo-first-order model [46]:

$$\frac{dQ_t}{dt} = k_1(Q_e - Q_t) \Rightarrow \lg(Q_e - Q_t) = \lg Q_e - \frac{k_1 t}{2.303} \quad (4)$$

Pseudo-second-order model [47]:

$$\frac{dQ_t}{dt} = k_2(Q_e - Q_t)^2 \Rightarrow \frac{t}{Q_t} = \frac{1}{k_2 Q_e^2} + \frac{t}{Q_e} \quad (5)$$

Intra-particle diffusion model [26]:

$$Q_t = k_{ip} t^{0.5} + C \quad (6)$$

...where:

k_1 (min^{-1}), k_2 (g·mg^{-1}·min^{-1}) – the rate constants of the pseudo-first-order kinetic model and the pseudo-second-order kinetic model, respectively;

k_{ip} (mg·g^{-1}·min$^{-0.5}$) – the rate constant

C (intercept) – a constant corresponding to an ideal boundary layer thickness.

The linear forms of these models were applied to fit the kinetic data (Fig. 3). The best-fit model was determined based on linear regression correlation coefficient values. Table 1 shows the kinetic parameters of the pseudo-first-order model and the pseudo-second-order model. The latter is more suitable to describe the kinetics process of ABB biosorption onto the adsorbent. The adsorption process is a multi-step process, mostly consisting of three consecutive stages. The applicability of the intra-particle diffusion model suggests that the sorption process of ABB onto *E. prolifera* was rather a complex process involving both the boundary layer (Step 1) and intra-particle diffusion (Step 2) [48]. Step 3 means the adsorption equilibrium. This phenomenon could indicate that intra-particle diffusion was not the only rate-controlling step, and other processes may affect the rate of sorption as well [49].

Effect of Initial pH

Both the ionic forms of the dye in solution and the surface electrical charge of the algae biomass depend on pH. Therefore, solution pH exerts a significant impact on both the biomass surface dye-binding sites and the dye chemistry in the medium [50-52]. In this study, dye biosorption experiments were conducted by shaking 0.025 g of the dried biomass in 100 ml dye solution (dye concentration 100 mg·L^{-1}) at the initial pH and for a period equal to the dye adsorption equilibrium time. As shown in Fig. 4, the equilibrium sorption capacity dramatically increased from 327.34 mg·g^{-1} at pH 2 to 357.22 mg·L^{-1}, then weakly fluctuated around 360 mg·L^{-1}.

As an anionic dye, ABB is first dissolved, and the sulfonate groups of the acid dye (D-SO_3Na) are dissociated and converted to anionic dye ions. Li et al. found that the isoelectric point (IEP) of *E. prolifera* was 4.4 [53]. When pH was less than 4.4, the biomass had positive surface charge due to the functional groups protonation, such as the hydroxyls and amines. High equilibrium sorption capacity obtained at lower pH values attributed to the electrostatic attractions between these positively charged cell surface and negatively charged dye anions. However, cellulose dissolved under acid conditions (pH=2~3) resulted in a number of decreases of function groups [54], which lead to the decline of sorption capacity. The amount of ABB adsorbed by *E. prolifera* plunged as the initial pH values dropped due to both the electrostatic attractions and cellulose, while the latter contributed more to this plunge. Thereafter, at higher pH, the alga polymeric components may get negatively charged (possible deprotonation), which went against the adsorption of anions. The value of pH decreased from 7.0 to 4.7 before and after adsorption, which indicates that *E. prolifera* is able to adjust the pH to a suitable adsorption level. During this process, heavy metals (Fe^{3+}, Cr^{2+}, Cr^{6+}, et al.) in acid dye or algae may also play an important role [55, 56]. When the dried biomass was suspended in this ABB solution, the hydroxide ions coordinated with the heavy metals and low pH.

The initial pH value of ABB simulated wastewater is 6.1. To guarantee a true examination of the *E. prolifera* adsorption property, all the following experiments were conducted without any pH value adjustment.

Effect of Adsorbent Dose

A range of 0.015- 0.05 g of biosorbent was mixed with 100 ml of the dye solution (i.e. 0.15-0.5 g·L^{-1}). Fig. 5 shows

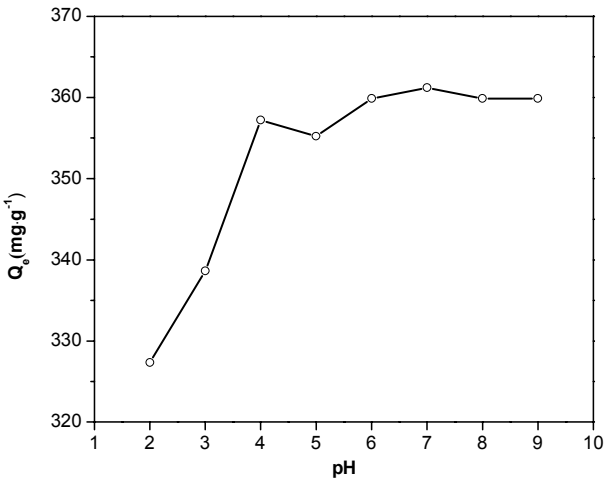

Fig. 4. The effect of pH values on the adsorption of ABB on dried *E. prolifera* (Conditions: C_0 = 100 mg·L^{-1}, adsorbent dose = 0.25 g·L^{-1}, temperature = 293 K, oscillation frequency = 150 rpm, contact time = 120 min).

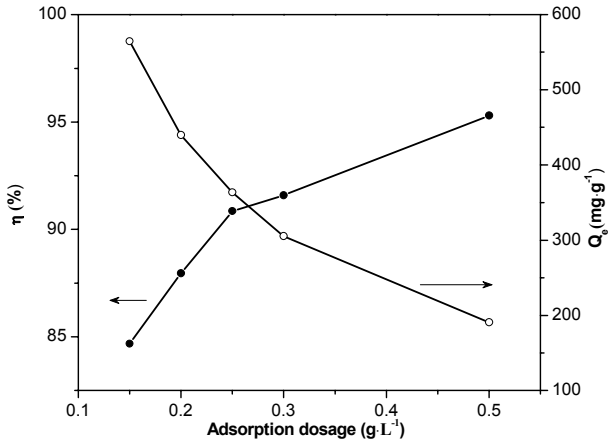

Fig. 5. Effect of sorption dosage on removal efficiency and sorption capacity of ABB (Conditions: C_0 = 100 mg·L^{-1}, temperature = 293 K, pH = 6.1, contact time = 120 min, oscillation frequency = 150 rpm).

that an increase in adsorbent dose at equilibrium time accompanying a descending trend in sorption capacity would lead to a weak ABB removal efficiency. Nevertheless, the removal efficiency values increased from 84.68% to 90.86%, as the adsorbent dose increased from 0.15 g·L^{-1} to 0.5g·L^{-1}, while the equilibrium adsorption capacity decreased from 546.53 mg·g^{-1} to 190.59 mg·g^{-1}. This trend is mostly attributed to an increase in the sorptive surface area and the availability of more active adsorption sites [57, 58]. When the biosorbent dose rose, the biosorbent surface area fell due to overlapping or aggregation, leading to the lower ABB equilibrium sorption capacity [59].

Effect of Oscillation Frequency

The oscillation frequency, a vital controlling parameter in the static adsorption process, influences both the dye molecules contact probability and the mass transfer processes [60]. The effect of oscillation frequency on dye removal efficiency during batch process was studied by changing the agitation speed from 0 to 200 rpm (Fig. 6). The dye concentration was 100 mg·L^{-1}. At the same time, the biosorbent dosage (0.25 g·L^{-1}) and exposure time (120 min) were kept constant. The dye removal efficiency increased with oscillation frequency up to 150 rpm, and then remained nearly constant (90.52%). When the oscillation frequency was under 100 rpm, the dried *E. prolifera* powder stacked together and the dispersiveness was inhomogeneous in dye solution, causing the descent of the solid-liquid interface. When the oscillation intensity was increased, the relative velocity between particles and liquid became larger, at which point the particle surface liquid film became thinner, reducing diffusion resistance [61]. Considering the energy consumption and adsorption efficiency, the appropriate oscillation frequency was set at 150 rpm.

Sorption Isotherm

Equilibrium data analysis provides priorities for comparing different biomaterials under different operational conditions and for designing and optimizing an operating procedure. The equilibrium sorption comparison was conducted at 283 K, 293 K, 303 K, 313 K, and 323 K, with varying adsorbent doses (0.15-0.5 mg·L^{-1}), fixed treatment time (120 min), and dye concentration (100 mg·L^{-1}). The data was modeled using the Langmuir and Freundlich equations (Eq. (7) and (8), respectively). Fig. 7 shows the raw data at five different temperature levels. The relevant parameters and correlation coefficients are in Table 2.

Langmuir: $$\frac{1}{Q_e} = \frac{1}{Q_{\max} K_L C_e} + \frac{1}{Q_{\max}} \quad (7)$$

Freundlich: $$\lg Q_e = \frac{1}{n} \lg C_e + \lg K_F \quad (8)$$

...where:

Q_e (mg·g^{-1}) – amount of adsorbed dye per unit weight of the algal adsorbent at equilibrium

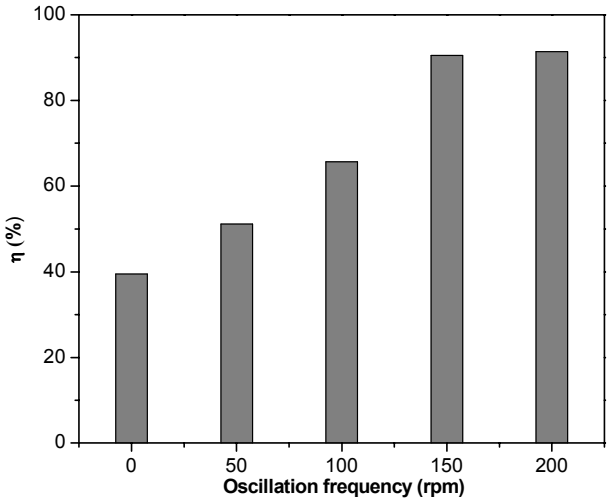

Fig. 6. Effect of oscillation frequency on the adsorption of ABB from aqueous solution (Conditions: C0 = 100 mg·L^{-1}, temperature = 293 K, adsorbent dose = 0.25 mg·L^{-1}, pH = 6.1, contact time =120 min).

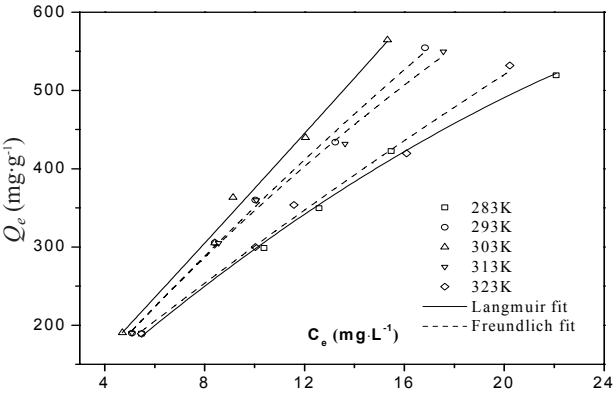

Fig. 7. Adsorption isotherms of ABB onto *E. prolifera* at 283, 293, 303, 313, and 323 K.

Table 2. Constants and correlation coefficient of Langmuir and Freundlich isotherm for ABB adsorption onto *E. prolifera*.

Temperature (K)	Langmuir isotherm				Freundlich isotherm		
	Q_{max} (mg·g^{-1})	K_L	R_L	R^2	K_F	n	R^2
283	1,111.11	0.21	0.05	0.9958	53.89	1.35	0.9966
293	3,333.33	0.45	0.02	0.9984	45.93	1.13	0.9966
303	3,333.33	0.44	0.02	0.9926	45.64	1.09	0.9920
313	2,500	0.38	0.03	0.9978	48.91	1.18	0.9948
323	1,428.57	0.26	0.04	0.9950	50.77	1.29	0.9932

Table 3. Comparison of the maximum sorption capacity of various types of dye by *E. prolifera* and other algae.

Algae	Adsorbate	Q_{max} (mg·g^{-1})	Reference
E. prolifera	ABB	3333.33	Present study
Enteromorpha spp.	Methylene Blue	273.73	[35]
E. prolifera	Acid Red 274	244.0	[6]
Spirogyra majuscula	Reactive Red 120	722.44	[34]
Spirodela polyrrhiza	Methylene Blue	144.93	[67]
Spirogyra I02	Direct Brown 1:1	0.9992	[33]
Azolla filiculoides	Acid Blue 15	116.28	[25]
Azolla filiculoides	Basic Orange	833.33	[26]
Caulerpa racemosa var. cylindracea	Methylene Blue	5.233	[29]
Caulerpa racemosa var. cylindracea	Malachite Green	25.67	[30]
Caulerpa lentillifera	Astrazon Blue FGRL	49.26	[27]
Caulerpa scalpelliformis	Sandocryl Golden Yellow C-2G	27	[51]
Caulerpa lentillifera	Astrazon Blue FGRL	38.9	[28]
	Astrazon Red GTLN	47.6	
	Methylene Blue	417	
Laminaria sp.	Reactive Black 5	100	[23]
Nostoc linckia	Reactive Red 198	93.5	[68]
Stoechospermum marginatum	Acid Orange II	14.95-71.05	[69]
Nizamuddin zanardini	Acid Black 1	29.79	[70]
Sargassum glaucescens	Acid Black 1	27.19	[70]
Stoechospermum marginatum	Acid Black 1	29.56	[70]

C_e (mg·L^{-1}) – equilibrium concentration of ABB
Q_{max} (mg·g^{-1}) – maximum monolayer adsorption capacity
K_L (L·g^{-1}) – Langmuir constants
K_F, n – Freundlich constants related to adsorption capacity and adsorption intensity, respectively.

In addition, one feature of the Langmuir equation can be defined in terms of a dimensionless constant known as separation factor (R_L). R_L can be calculated by using Eq. (9) [34, 62].

$$R_L = \frac{1}{1 + K_L C_0} \quad (9)$$

...where:
C_0 (100 mg·L^{-1}) – initial dye concentration
K_L (L·g^{-1}) – Langmuir constants
R_L value indicates the adsorption process is irreversible when R_L is 0; favorable when R_L is between 0 and 1; linear when R_L is 1; and unfavorable when R_L is greater than 1 [63, 64].

Table 4. Thermodynamic parameters for adsorption of ABB on dried *E. prolifera* powder.

Temperature (K)	K_C	ΔH^0 (kJ·mol^{-1})	ΔS^0 (kJ·mol^{-1}·K^{-1})	ΔG^0 (kJ·mol^{-1})
303	9.938	-10.676	-0.016	-5.785
313	8.931			-5.698
323	7.639			-5.460

Both the Langmuir and Freundlich models could explain the adsorption based on R^2 values (Table 2), indicating that adsorption in the range of concentration should still be within the monolayer region [27]. Despite increasing the dye concentration, which could result in a more significant difference between the two models, sorption isotherm studies could be suitable for describing the adsorption processes given the low probability of reaching 100 mg·L^{-1} concentration for conventional textile wastewater.

The Langmuir parameters, i.e., Q_{max} and K_L experienced a growth from the temperature of 283 K to 293 K, while decreased at 303 K and above. A similar phenomenon was also found by Lee et al. [65] and Marungrueng et al. [27]. High temperatures would increase the kinetic energy mobility of the dye and hence enhance the mobility of the dye ions. This could be used to explain a higher chance of the dye being adsorbed onto the adsorbent and its increasing Q_{max} and K_L at lower temperature. The adsorbent may contribute to desorption of dye ions since the diffusion is an exothermic process at higher temperature levels. Thus the range of 303 K to 313 K was the best in the investigation area. The Q_{max} predicted by the Langmuir equation dropped from 3,333.33 mg·g^{-1} at 303-313 K to 1,428.57 mg·g^{-1} at 323 K. Moreover, all R_L values at different temperatures ranged between 0.02 and 0.05 confirm that the adsorption process is favorable (Table 2). A similar tendency was reported in a previous study [6]. The Freundlich exponent 1/n was smaller than 1, which also reflected favorable adsorption [66].

In addition, the adsorption capacities of various types of algae for the reactive dyes sorption were summarized in Table 3, among which the adsorption capacity of the alga in this study is the highest available. It is noteworthy that *E. prolifera* employed for ABB removal works more effectively than Methylene Blue and Acid Red 274 dislodgment. This may be due to the difference of dyes. Furthermore, *E. prolifera* is available in large quantities, and sometimes its bloom even becomes a disaster in Qingdao, China. Generally, the large monolayer adsorption capacity rendered the alga a promising biosorbent for color removal, especially from dye-containing effluent from the textile industry.

Adsorption Thermodynamic

Thermodynamic parameters associated with the adsorption, viz. standard Gibbs free energy change (ΔG^0), standard enthalpy change (ΔH^0), and standard entropy change (ΔS^0), were calculated. The standard Gibbs free energy change for sorption of ABB onto *E. prolifera* is estimated by using equilibrium constant K_C and written as:

$$\Delta G^0 = -RT\ln K_C \tag{10}$$

The standard enthalpy change (kJ·mol^{-1}) and the standard entropy change of adsorption (kJ·mol^{-1}·K^{-1}) were calculated from van't Hoff equation as follows [30]:

$$\ln K_C = -\frac{\Delta H^0}{RT} + \frac{\Delta S}{R} \tag{11}$$

...where:

K_C – equilibrium constant for sorption

R – the universal gas constant (8.314 J·mol^{-1}·K^{-1})

T – the temperature in Kelvin.

The K_C value was determined by Eq. (12).

$$K_C = \frac{C_s}{C_e} \tag{12}$$

...where: C_s (mg·L^{-1}) is the amount of ABB sorbed on *E. prolifera* at equilibrium, C_e (mg·L^{-1}) is the equilibrium concentration of ABB in solution.

At different temperatures, the same adsorbent dosage (0.25 g·L^{-1}) and equilibrium time (120 min) were selected; firstly C_e and then C_s and K_C were determined [51].

The values of ΔH^0 and ΔS^0 could be obtained from the slop and intercept of a plot of $\ln K_C$ against 1/T (Fig. 8 with R=0.99). The calculated values of thermodynamic parameters are shown in Table 4.

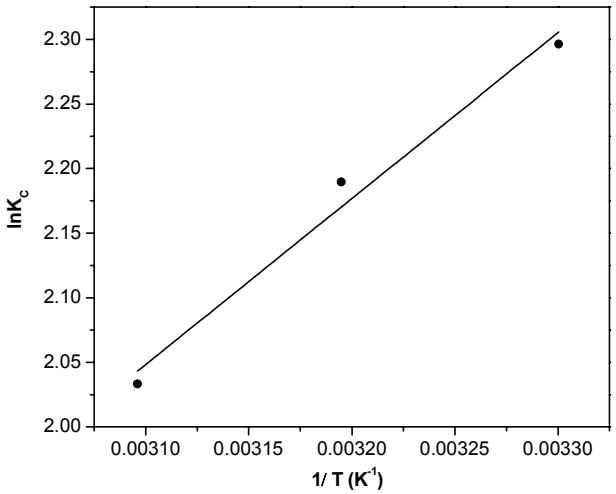

Fig. 8. Plot of $\ln K_C$ versus 1/T for ABB for the determination of adsorption enthalpy.

The K_C indicates the capability of the biomass to retain dye molecules and also the extent of its movement in a solution phase [71]. According to Choi et al. and Özer et al., K_C value decreased as the temperature rose, resulting in a shift of the adsorption equilibrium to the left [6, 72]. The negative values of ΔG^0 confirm the feasibility of the process and the spontaneous nature of biosorption with a high preference of ABB on *E. prolifera*. Furthermore, the absolute magnitude of the change in free energy for physisorption is between -20 and 0 kJ·mol^{-1} and chemisorption has a range of -80 to -400 kJ·mol^{-1}. ΔG^0 values are -5.785 kJ·mol^{-1}, -5.698 kJ·mol^{-1} and -5.460 kJ·mol^{-1} for 303 K, and 313 K and 323 K, respectively. These results demonstrate physisorption for the sorption process. The negative value of change in enthalpy (ΔH^0) showed the adsorption is exothermic in nature. The negative value of change in entropy (ΔS^0) reflects the decreased randomness at the solid/solution interface during the adsorption of dye on dried *Enteromorpha prolifera* powder.

Conclusions

ABB removal from aqueous solution through biosorption onto dried *E. prolifera* powder was investigated. Green algae have been, for the first time, employed in study for ABB biosorption. The adsorption method is simple and the adsorbents have shown great potential for the removal of acid dyes. The main conclusions drawn from the above study are summatized below:

(1) The treatment conditions for dye concentration 100 mg·L^{-1} were optimized: pH value 4~9, water temperature 303~313 K, adsorbent dosage 0.25 g·L^{-1} and oscillation frequency 150 rpm.

(2) The biosorption equilibrium could be defined by both the Langmuir isotherm model and Freundlich model. The maximum equilibrium sorption was 1,111.11-3,333.33 mg·L^{-1} at 293 and 303 K.

(3) Sorption dynamic study revealed that the sorption process followed the pseudo-second-order equation; the sorption process was complex, both the boundary of liquid film and intra-particle diffusion contributed to the rate-determining step.

(4) Thermodynamic parameters showed that the sorption process of ABB onto *E. prolifera* is exothermic, spontaneous, and physisorption.

(5) Considering the data and analysis presented in this paper, it is suggested that *E. prolifera* could be greatly appropriate for the detoxification of reactive dye-bearing industrial effluents.

Acknowledgements

The authors gratefully acknowledge the financial support from the National Marine Public Welfare Research Project (No. 201005012, China). Sincere thanks are given to the reviewers for their valuable comments to improve the paper.

References

1. DEMIRBAS A., Agricultural based activated carbons for the removal of dyes from aqueous solutions: a review. J. Hazard. Mater. **167**, 1, **2009**.
2. RAFATULLAH M., SULAIMAN O., HASHIM R., AHMAD A. Adsorption of methylene blue on low-cost adsorbents: a review. J. Hazard. Mater. **177**, 70, **2010**.
3. CELEKLI A., GEYIK F. Artificial neural networks (ANN) approach for modeling of removal of Lanaset Red G on *Chara contraria*. Bioresour. Technol. **102**, 5634, **2011**.
4. MCMULLAN G., MEEHAN C., CONNEELY A., KIRBY N., ROBINSON T., NIGAM P., BANAT I.M., MARCHANT R., SMYTH W.F. Microbial decolourisation and degradation of textile dyes. Appl. Microbiol. Biotechnol. **56**, 81, **2001**.
5. PEARCE C.I., LLOYD J.R., GUTHRIE J.T. The removal of colour from textiles wastewater using whole bacterial cells: a review. Dyes Pigments. **58**, 179, **2003**.
6. ÖZER A., AKKAYA G., TURABIK M. Biosorption of Acid Red 274 (AR 274) on *Enteromorpha prolifera* in a batch system. J. Hazard. Mater. **126**, 119, **2005**.
7. LEE J.W., CHOI S.P., THIRUVENKATACHARI R., SHIM W.G., MOON H. Evaluation of the performance of adsorption and coagulation processes for the maximum removal of reactive dyes. Dyes Pigments. **69**, 196, **2006**.
8. BANAT I.M., NIGAM P., SINGH D., MARCHANT R. Microbial decolourization of textile-dye-containing effluents: a review. Bioresour. Technol. **58**, 217, **1996**.
9. SLOKAR Y.M., MAJCEN LE MARECHAL A. Methods of decoloration of textile wastewaters. Dyes Pigments. **37**, 335, **1998**.
10. DELEE W., O'NEILL C., HAWKES F.R., PINHEIRO H.M. Anaerobic treatment of textile effluents: a review. J. Chem. Bioresour. Technol. **73**, 323, **1998**.
11. ROBINSON T., MCMULLAN G., MARCHANT R., NIGAM P. Remediation of dyes in textiles effluent: a critical review on current treatment technologies with a proposed alternative. Bioresour. Technol. **77**, 247, **2001**.
12. CRINI G. Non-conventional low-cost adsorbents for dye removal: a review. Bioresour. Technol. **97**, 1061, **2006**.
13. GUPTA V.K. Application of low-cost adsorbents for dye removal-a review. J. Environ. Manage. **90**, 2313, **2009**.
14. SALLEH M.A.M., MAHMOUD D.K., KARIM W.A.W.A., IDRIS A. Cationic and anionic dye adsorption by agricultural solid wastes: A comprehensive review. Desalination. **280**, 1, **2011**.
15. SRINIVASAN A., VIRARAGHAVAN T. Decolorization of dye wastewaters by biosorbents: a review. Environ. Manage. **91**, 1915, **2010**.
16. NOROOZI B., SORIAL G.A., BAHRAMI H., ARAMI M. Equilibrium and kinetic adsorption study of a cationic dye by a natural adsorbent-Silkworm pupa. J. Hazard. Mater. **139**, 167, **2007**.
17. SRIVASTAVA V.C., MALL I.D., MISHRA I.M. Adsorption thermodynamics and isosteric heat of adsorption of toxic metal ions onto bagasse fly ash (BFA) and rice husk ash (RHA). Chem. Eng. J. **132**, 267, **2007**.
18. FU Y., VIRARAGHAVAN T. Fungal decolorization of dye wastewaters: a review. Bioresour. Technol. **79**, 251, **2001**.
19. WON S.W., CHOI S.B., YUN Y.S. Interaction between protonated waste biomass of *Corynebacterium glutamicum* and anionic dye Reactive Red 4. Colloids Surf., A. **262**, 175, **2005**.

20. VENKATA MOHAN S., CHANDRASEKHAR RAO N., KRISHNA PRASAD K., KARTHIKEYAN J. Treatment of simulated Reactive Yellow 22 (azo) dye effluents using Spirogyra species. Waste Manage. **22**, 575, **2002**.
21. CRINI G., BADOT P.M. Application of chitosan, a natural aminopolysaccharide, for dye removal from aqueous solutions by adsorption processes using batch studies: a review of recent literature. Prog. Polym. Sci. **33**, 399, **2008**.
22. RAMAKRISHNA K.R., VIRARAGHAVAN T. Dye removal using peat. Am. Dye. Rep. **85**, 28, **1996**.
23. VIJAYARAGHAVAN K., YUN Y.S. Biosorption of C.I. Reactive Black 5 from aqueous solution using acid-treated biomass of brown seaweed *Laminaria* sp.. Dyes Pigments. **76**, 726, **2008**.
24. RUBIN E., RODRIGUEZ P., HERRERO R., CREMADES J., BARBARA I., SASTRE DE VICENTE M.E. Removal of Methylene Blue from aqueous solutions using as biosorbent *Sargassum muticum*: an invasive macroalga in Europe. J. Chem. Bioresour. Technol. **80**, 291, **2005**.
25. PADMESH T.V.N., VIJAYARAGHAVAN K., SEKARAN G., VELAN M. Biosorption of Acid Blue 15 using fresh water macroalga *Azolla filiculoides*: Batch and column studies. Dyes Pigments. **71**, 77, **2006**.
26. TAN C., LI G., LU X.Q., CHEN Z. Biosorption of Basic Orange using dried *A. filiculoides*. Ecol. Eng. **36**, 1333, **2010**.
27. MARUNGRUENG K., PAVASANT P. Removal of basic dye (Astrazon Blue FGRL) using macroalga *Caulerpa lentillifera*. Environ. Manage. **78**, 268, **2006**.
28. MARUNGRUENG K., PAVASANT P. High performance biosorbent (*Caulerpa lentillifera*) for basic dye removal. Bioresour. Technol. **98**, 1567, **2007**.
29. CENGIZ S., CAVAS L. Removal of methylene blue by invasive marine seaweed: *Caulerpa racemosa* var. *cylindracea*. Bioresour. Technol. **99**, 2357, **2008**.
30. BEKÇI Z., SEKI Y., CAVAS L. Removal of malachite green by using an invasive marine alga *Caulerpa racemosa* var. *cylindracea*. J. Hazard. Mater. **16**, 1454, **2009**.
31. ÖZER A., AKKAYA G., TURABIK M. Biosorption of Acid Blue 290 (AB 290) and Acid Blue 324 (AB 324) dyes on *Spirogyra rhizopus*. J. Hazard. Mater. **135**, 355, **2006**.
32. ARICA M.Y., BAYRAMOGLU G. Biosorption of reactive red-120 dye from aqueous solution by native and modified fungus biomass preparations of *Lentinus sajor-caju*. J. Hazard. Mater. **149**, 499, **2007**.
33. MOHAN S.V., RAMANAIAH S.V., SARMA P.N. Biosorption of direct azo dye from aqueous phase onto *Spirogyra* sp. I02: Evaluation of kinetics and mechanistic aspects. Biochem. Eng. J. **38**, 61, **2008**.
34. CELEKLI A., YAVUZATMACA M., BOZKURT H. Kinetic and equilibrium studies on the adsorption of reactive red 120 from aqueous solution on *Spirogyra majuscule*. Chem. Eng. J. **152**, 139, **2009**.
35. NCIBI M.C., HAMISSA A.M., FATHALLAH A., KORTAS M.H., BAKLOUTI T., MAHJOUB B., SEFFEN M. Biosorptive uptake of methylene blue using Mediterranean green alga *Enteromorpha* spp.. J. Hazard. Mater. **170**, 1050, **2009**.
36. CALLOW M.E., CALLOW J.A., PICKETT-HEAPS J.D., WETHERBEE R. Primary adhesion of *Enteromorpha* (*Chlorophyta*, *Ulvales*) propagules: quantitative settlement studies and video microscopy. J Phycol. **33**, 938, **1997**.
37. HIRAOKA M., OHNO M., KAWAGUCHI S., YOSHIDA G. Crossing test among floating *Ulva* thalli forming 'green tide' in Japan. Hydrobiologia. **512**, 239, **2004**.
38. RAKHSHAEE R., KHOSRAVI M., GANJI M.T. Kinetic modeling and thermodynamic study to remove Pb(II), Cd(II), Ni(II) and Zn(II) from aqueous solution using dead and living *Azolla filiculoides*. J. Hazard. Mater. **134**, 120, **2006**.
39. SARI A., TUZEN M. Biosorption of cadmium(II) from aqueous solution by red algae (*Ceramium virgatum*): equilibrium, kinetic and thermodynamic studies. J. Hazard. Mater. **157**, 448, **2008**.
40. CHANDRASEKHAR S., PRAMADA P.N. Rice husk ash as an adsorbent for methylene blue–effect of ashing temperature. Adsorption. **12**, 27, **2006**.
41. BALARIA A., SCHIEWER S. Assessment of biosorption mechanism for Pb binding by citrus pectin. Sep. Purif. Technol. **63**, 577, **2008**.
42. SUGANUMA S., NAKAJIMA K., KITANO M., YAMAGUCHI D., KATO H., HAYASHI S. Hydrolysis of cellulose by amorphous carbon bearing SO_3H, COOH, and OH groups. J. Am. Chem. Soc. **130**, 12787, **2008**.
43. MOHANTY K., JHA M., MEIKAP B.C., BISWAS M.N. Biosorption of Cr (VI) from aqueous solution by *Eichhornia crassipes*. Chem. Eng. J. **117**, 71, **2006**.
44. AKSU Z., TATLI A.I., TUNÇ Ö. A comparative adsorption/biosorption study of Acid Blue 161: Effect of temperature on equilibrium and kinetic parameters. Chem. Eng. J. **42**, 23, **2008**.
45. SARKAR M., ACHARYA P.K., BHATTACHARYA B. Modeling the adsorption kinetics of some priority organic pollutants in water from diffusion and activation energy parameters. J. Colloid Interface Sci. **266**, 28, **2003**.
46. LAGERGREN S. About the theory of so-called adsorption of soluble substances. Kungliga Svenska Vetenskapsakademiens. Handlingar, Band. **24**, 1, **1898**.
47. HO Y.S., MCKAY G. Pseudo-second order model for sorption processes. Process Biochem. **34**, 451, **1999**.
48. GOPAL V., ELANGO K.P. Equilibrium, kinetic and thermodynamic studies of adsorption of fluoride onto plaster of Paris. J. Hazard. Mater. **141**, 98, **2007**.
49. YAO R., MENG F., ZHANG L., MA D., WANG M. Defluoridation of water using neodymium-modified chitosan. J. Hazard. Mater. **165**, 454, **2009**.
50. FU Y., VIRARAGHAVAN T. Dye biosorption sites in *Aspergillus niger*, Bioresour. Technol. **82**, 139, **2002**.
51. ARAVINDHAN R., RAO J.R., NAIR B.U. Removal of basic yellow dye from aqueous solution by sorption on green alga *Caulerpa scalpelliformis*. J. Hazard. Mater. **142**, 68, **2007**.
52. KUMAR K.V., PORKODI K. Mass transfer, kinetics and equilibrium studies for the biosorption of methylene blue using *Paspalum notatum*. J. Hazard. Mater. **146**, 214, **2007**.
53. LI Y., DU Q., WANG X., ZHANG P., WANG D., WANG Z., XIA Y. Removal of lead from aqueous solution by activated carbon prepared from *Enteromorpha prolifera* by zinc chloride activation. J. Hazard. Mater. **183**, 583, **2010**.
54. DAWSEY T.R., MCCORMICK C.L. The lithium chloride/dimethylacetamide solvent for cellulose: a literature review. J. Macromol. Sci., Rev. Macromol. Chem. Phys. **30**, 405, **1990**.
55. NETPRADIT S., THIRAVETYAN P., TOWPRAYOON S. Application of 'waste' metal hydroxide sludge for adsorption of azo reactive dyes. Water Res. **37**, 763, **2003**.
56. NETPRADIT S., THIRAVETYAN P., TOWPRAYOON S. Evaluation of metal hydroxide sludge for reactive dye adsorption in a fixed-bed column system. Water Res. **38**, 71, **2004**.

57. GARG V.K., AMITA M., KUMAR R., GUPTA R. Basic dye (methylene blue) removal from simulated wastewater by adsorption using Indian Rosewood sawdust: a timber industry waste. Dyes pigments. **63**, 243, **2004**.
58. HO Y.S., CHIANG C.C. Sorption studies of acid dye by mixed sorbents. Adsorption. **7**, 139, **2001**.
59. NUHOGLU Y., MALKOC E., GÜRSES A., CANPOLAT N. The removal of Cu (II) from aqueous solutions by *Ulothrix zonata*, Bioresour Technol. **85**, 331, **2002**.
60. MENG F., LI Y., ZHOU Y., DU X. Static and dynamic adsorption of fluoride using La(lll)-loaded chitosan beads crosslinked with EGDE. China Chem. Ind. Eng. Soc. J. **62**, 3192, **2011**.
61. CHEUNG W.H., SZETO Y.S., MCKAY G. Intraparticle diffusion processes during acid dye adsorption onto chitosan. Bioresour. Technol. **98**, 2897, **2007**.
62. MCKAY G. Adsorption of dyestuffs from aqueous solutions with activated carbon I: Equilibrium and batch contact-time studies. J. Chem. Technol. Biotechnol. **32**, 759, **1982**.
63. LEECHART P., NAKBANPOTE W., THIRAVETYAN P. Application of 'waste' wood-shaving bottom ash for adsorption of azo reactive dye. Journal of Environ. Manage. **90**, 912, **2009**.
64. ALKAN M., DEMIRBAŞ Ö., DOĞAN M., ARSLAN O. Surface properties of bovine serum albumin-adsorbed oxides: Adsorption, adsorption kinetics and electrokinetic properties. Microporous Mesoporous Mater. **96**, 331, **2006**.
65. LEE C.K., LOW K.S., CHOW S.W. Chrome sludge as an adsorbent for colour removal, Environ. Technol. **17**, 1023, **1996**.
66. SEKI Y., YURDAKOÇ K. Adsorption of Promethazine hydrochloride with KSF Montmorillonite. Adsorption. **12**, 89, **2006**.
67. WARANUSANTIGUL P., POKETHITIYOOK P., KRUATRACHUE M., UPATHAM E.S. Kinetics of basic dye (methylene blue) biosorption by giant duckweed (*Spirodela polyrrhiza*). Environ. Pollut. **125**, 385, **2003**.
68. MONA S., KAUSHIK A., KAUSHIK C.P. Biosorption of reactive dye by waste biomass of *Nostoc linckia*. Ecol. Eng. **37**, 1589, **2011**.
69. KOUSHA M., DANESHVAR E., SOHRABI M.S., JOKAR M., BHATNAGAR A. Adsorption of acid orange II dye by raw and chemically modified brown macroalga *Stoechospermum marginatum*. Chem. Eng. J. **192**, 67, **2012**.
70. KOUSHA M., DANESHVAR E., DOPEIKAR H., TAGHAVI D., BHATNAGAR A. Box-Behnken design optimization of Acid Black 1 dye biosorption by different brown macroalgae. Chem. Eng. J. **179**, 158, **2012**.
71. REDDY M.R., DUNN S.J. Distribution coefficients for nickel and zinc in soils. Environ. Pollut. **11**, 303, **1986**.
72. CHOI Y.S., CHO J.H. Color removal from dye wastewater using vermiculite. Environ. Technol. **17**, 1169, **1996**.